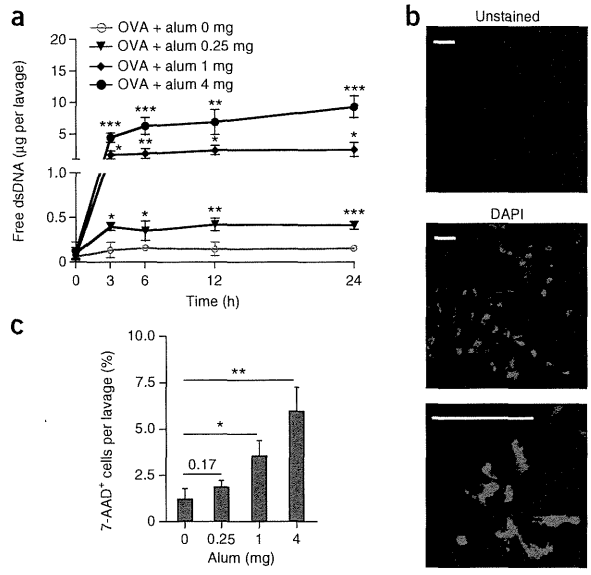

Figure 1 Alum induces cell death and release of host DNA at sites of injection. (**a**) Quantity of free dsDNA in the acellular fraction of the peritoneal lavage fluid of mice treated i.p. with increasing doses of alum, measured over time using quantitative fluorescent dsDNA stain. (**b**) Confocal microscopic imaging of extracellular DNA deposition in alum macroscopic i.p. depots stained with 4′,6-diamidino-2-phenylindole (DAPI). Scale bars, 25 μm. (**c**) Cell death rate in the peritoneal lavage fluid of mice treated i.p. with increasing doses of alum, assessed by staining with 7-aminoactinomycin D (7-AAD) and flow cytometry. $n = 5$ (**a**,**c**). Data are representative of one of three independent experiments. Error bars show means ± s.d. $^{*}P < 0.05$, $^{**}P < 0.01$, $^{***}P < 0.001$.

that was abrogated by DNase I treatment of the lavage fluid prior to transfer (**Supplementary Fig. 3a**,**b**).

We also observed that the proliferation of both adoptively transferred carboxyfluorescein succinimidyl ester (CFSE)-labeled (**Fig. 2g**) and endogenous (**Supplementary Fig. 4**) OVA-specific $CD4^+$ T cells was comparable in OVA and DNA– and OVA and alum–treated mice and reduced after treatment of the mice with DNase I (**Fig. 2g** and **Supplementary Fig. 4**). These results thus support the idea that host DNA is a potent endogenous adjuvant molecule that has a role in the induction of humoral and T cell responses by alum.

Alum signals through Tbk1 and Irf3 to boost IgE responses

In vivo, only toll-like receptor 9 (Tlr9) has been implicated in host DNA recognition, under specific pathologic conditions[18,19]. However, we observed that mice deficient in Tlr9 developed humoral responses similar to those of their wild-type (WT) counterparts in response to alum immunization (data not shown).

In addition to Tlr9, other molecules have been identified as putative host DNA receptors *in vitro*[20–27]. These receptors activate either the inflammasome pathway, leading to mature IL-1β protein expression[21,23,24], or the Irf3 pathway, leading to interferon (IFN)-β1 expression[20,22,25–28]. Whereas OVA and DNA upregulated IFN-β1 secretion similarly to OVA and alum (**Fig. 3a**), OVA and DNA did not induce more IL-1β production than OVA alone, unlike OVA and alum (**Fig. 3b**). This suggested that, after alum immunization, extracellular DNA activated Irf3, but not the inflammasome pathway. By further investigating the general importance of inflammasomes

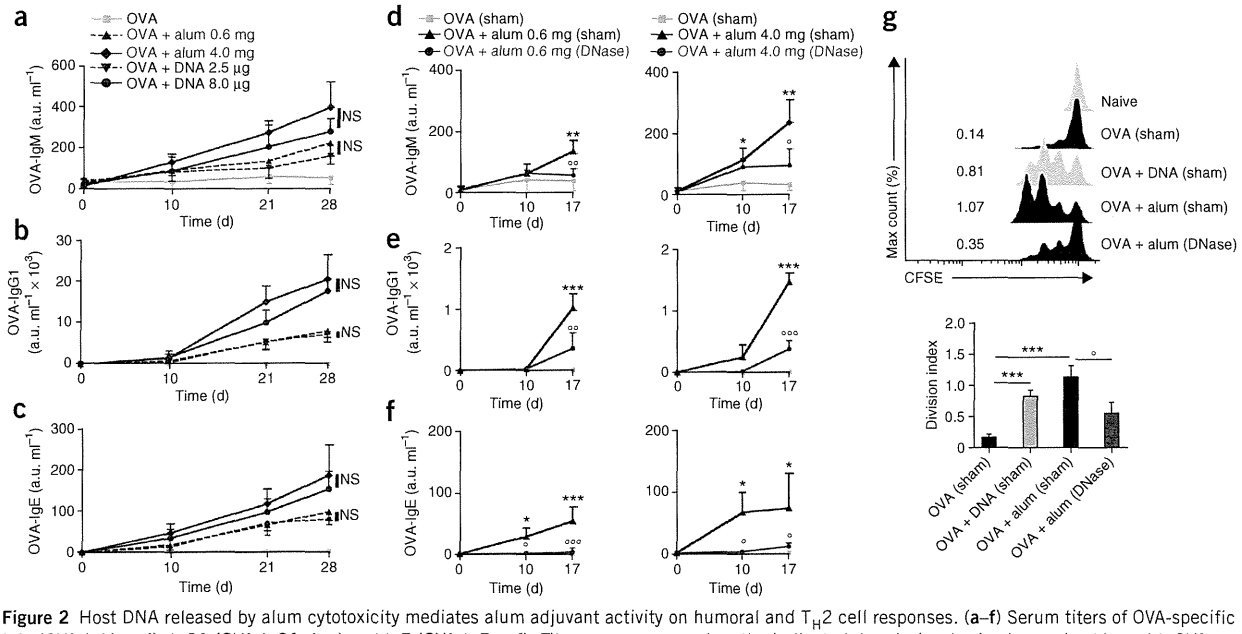

Figure 2 Host DNA released by alum cytotoxicity mediates alum adjuvant activity on humoral and T_H2 cell responses. (**a**–**f**) Serum titers of OVA-specific IgM (OVA-IgM; **a**,**d**), IgG1 (OVA-IgG1; **b**,**e**) and IgE (OVA-IgE; **c**,**f**). Titers were measured on the indicated days in (**a**–**c**) mice immunized i.p. with OVA alone, OVA and alum, or OVA and DNA on days 0 and 14, and boosted with OVA on d 21; or in (**d**–**f**) mice immunized i.p. with OVA or OVA and alum, treated i.p. with DNase I both 3 and 18 h later, and then boosted with OVA 10 d later. (**g**) Proliferation profile (top) and division index (bottom) of adoptively transferred CFSE-labeled OVA-specific $CD4^+$ OT-II cells in the bronchial lymph nodes of mice treated i.p. with OVA, OVA and DNA, OVA and alum, or OVA and alum followed by DNase I treatment. Inserted numbers indicate division index values. $n = 5$; data are representative of one of two (**a**–**c**) or three (**d**–**g**) independent experiments. Error bars show means ± s.d. *, OVA versus OVA and adjuvant; °, OVA and alum versus OVA and alum followed by DNase I treatment; $^{*,\circ}P < 0.05$, $^{**,\circ\circ}P < 0.01$, $^{***,\circ\circ\circ}P < 0.001$. a.u., arbitrary unit. NS, not significant.

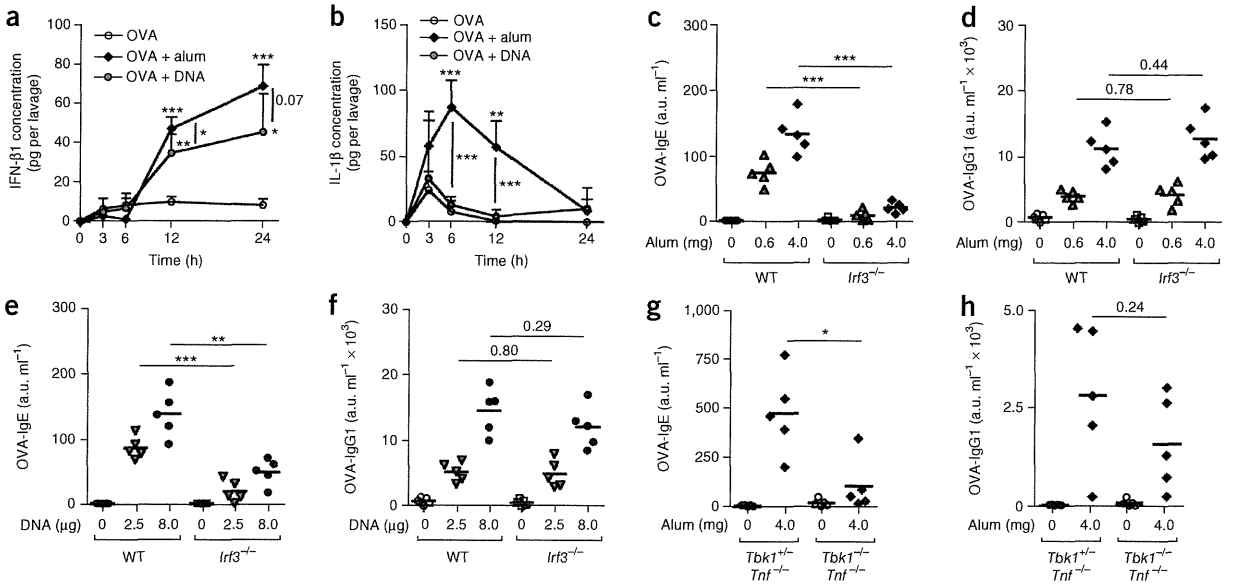

Figure 3 Alum and host genomic DNA trigger type I IFN secretion and IgE responses through activation of the Tbk1-Irf3 axis. (**a**,**b**) Quantities of (**a**) IFN-β1 and (**b**) IL-1β in the peritoneal lavage fluid over time by ELISA in WT mice treated i.p. with OVA, OVA and DNA, or OVA and alum. (**c**–**f**) Serum titers of OVA-specific IgE (**c**,**e**) and IgG1 (**d**,**f**) measured on day 28 in WT and *Irf3*$^{-/-}$ mice immunized i.p. with OVA, OVA and alum (**c**,**d**), or OVA and DNA (**e**,**f**) on days 0 and 14, and then boosted with OVA on day 21. (**g**,**h**) Serum titers of OVA-specific IgE (**g**) and IgG1 (**h**) measured on day 28 in *Tbk1*$^{+/-}$/*Tnf*$^{-/-}$ and *Tbk1*$^{-/-}$/*Tnf*$^{-/-}$ mice immunized i.p. with OVA and alum on days 0 and 14, and then boosted with OVA on day 21. $n = 5$; data are representative of one of three independent experiments. Error bars show means ± s.d. $^{*}P < 0.05$, $^{**}P < 0.01$, $^{***}P < 0.001$. a.u., arbitrary unit.

in the adjuvant activity of alum, we observed that Nlrp3-deficient (*Nlrp3*$^{-/-}$) and Caspase 1–deficient (*Casp1*$^{-/-}$) mice developed humoral responses comparable to those of WT mice after alum immunization (**Supplementary Fig. 5a**,**b**).

We next examined whether Irf3 is required for the adjuvant activity of alum. We found that, compared with their WT counterparts, in Irf3-deficient (*Irf3*$^{-/-}$) mice, i.p. immunization with OVA and alum triggered reduced antigen-specific IgE responses (**Fig. 3c**). Notably, however, the antigen-specific IgG1 serum titers of *Irf3*$^{-/-}$ mice were similar to those of WT mice (**Fig. 3d**). Furthermore, we also saw the dependency of antigen-specific IgE production on Irf3 when we used human serum albumin (HSA) in place of OVA and Alhydrogel in place of alum (**Supplementary Fig. 6a**). We obtained similar results when we administered OVA and alum i.m. rather than i.p. (**Supplementary Fig. 7a**). IgG1 production remained unaffected in *Irf3*$^{-/-}$ mice under these different conditions (**Supplementary Fig. 6b** and **Supplementary Fig. 7b**). We also observed a reduction in the production of antigen-specific IgE, but not of IgG1, when we immunized *Irf3*$^{-/-}$ mice i.p. or i.m. with OVA and DNA in place of OVA and alum (**Fig. 3e**,**f** and **Supplementary Fig. 7c**,**d**), supporting the notion that both alum and host DNA induce IgE responses through the same pathway.

Most of the host DNA–activated pathways that lead to Irf3 activation signal through TANK-binding kinase 1 (Tbk1)[20,22,25,28]. Tbk1-deficient mice (*Tbk1*$^{-/-}$) die *in utero* from massive liver apoptosis, but a combined deficiency for tumor necrosis factor (encoded by *Tnf*) avoids these lethal effects[28,29]. We found that immunized *Tbk1*/*Tnf* double-knockout mice developed reduced OVA-specific IgE responses (**Fig. 3g**) but similar OVA-specific IgG1 serum titers (**Fig. 3h**) when compared to immunized control *Tbk1*$^{+/-}$/*Tnf*$^{-/-}$ mice, thereby suggesting a role for the Tbk1-Irf3 axis in the adjuvant activity of alum on IgE responses.

The only currently known mammalian DNA-sensitive pathways able to activate the Tbk1-Irf3 axis involve the sensing of genomic DNA by Sting (a stimulator of IFN genes)[25], and the activation of Ddx58 (DEAD box polypeptide 58) by RNA transcribed from DNA by polymerase III (ref. 22). Both Sting and Ddx58 act upstream of mitochondrial antiviral signaling protein (encoded by *Mavs*) to activate Tbk1 and Irf3 (refs. 22,25). We observed that OVA and alum–immunized *Mavs*$^{-/-}$ mice developed OVA-specific IgE and IgG1 serum titers similar to those of WT mice (data not shown). Zbp1 (Z-DNA binding protein 1, also called Dai) has also been proposed as a cytoplasmic DNA sensor *in vitro*[20], although its role remains unclear *in vivo*[30]. *Zbp1*$^{-/-}$ mice did not show reduced antigen-specific IgE or IgG1 production in response to OVA and alum immunization in comparison with WT mice (data not shown).

Together, these results indicate that alum-induced host DNA release promotes IgG1 and IgE responses through distinct signaling pathways that do not depend on currently identified DNA receptors. They also identify Irf3 as an essential mediator of IgE production after alum immunization.

Irf3 is essential for alum-boosted canonical T_H2 responses

Given that IgE isotype switching by B cells is best induced by T cells expressing a T_H2 cytokinic profile, we suspected that Irf3 deficiency would have an effect on T_H2 cell responses after alum immunization. Indeed, the proliferation of transferred CFSE-labeled OVA-specific CD4^{+} cells (**Fig. 4a**), the differentiation of endogenous antigen-specific T_H2 cells (**Supplementary Fig. 8a**,**b**) and the secretion of T_H2 cytokines in response to OVA re-stimulation (**Fig. 4b**) were reduced in the bronchial lymph nodes (BLNs) of *Irf3*$^{-/-}$ mice injected i.p. with OVA and DNA or with OVA and alum. Furthermore, in a classical asthma model based on OVA and alum sensitization followed by

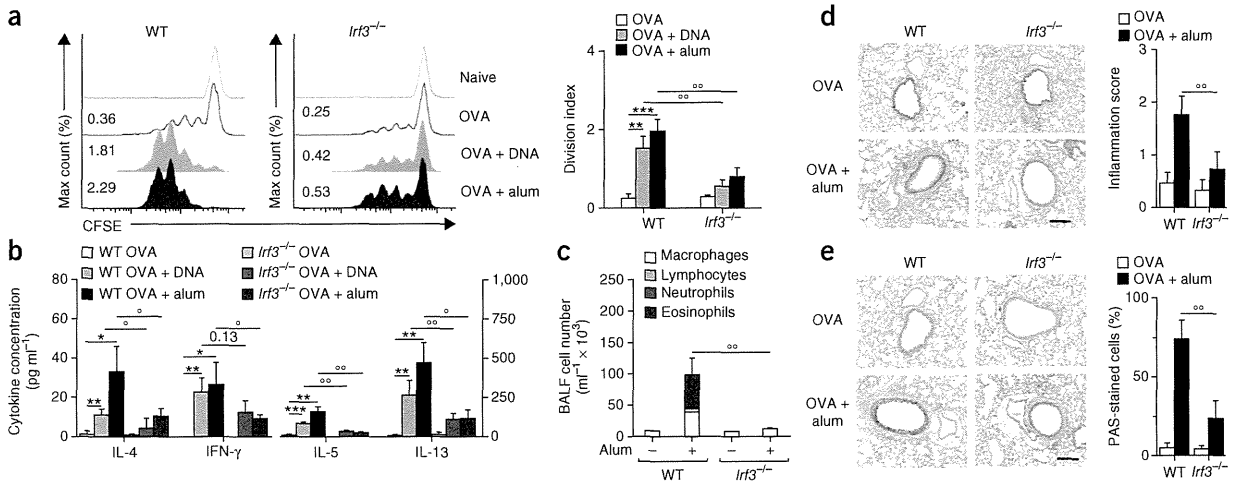

Figure 4 Irf3 is essential for the boosting of canonical T_H2 cells by alum and genomic DNA. (**a**) Proliferation profile (left) and division index (right) of adoptively transferred OVA-specific CD4+ OT-II cells in the BLNs of WT and *Irf3*$^{-/-}$ mice treated i.p. with OVA, OVA and DNA, or OVA and alum. Inserted numbers indicate division index values. (**b**) Cytokine concentrations in the supernatant of OVA-stimulated BLN cells isolated from WT and *Irf3*$^{-/-}$ mice treated with OVA, OVA and DNA, or OVA and alum. (**c–e**) Assessment of allergic airway inflammation in OVA- or OVA and alum–sensitized WT and *Irf3*$^{-/-}$ mice challenged with aerosolized OVA. (**c**) Total and differential immune cell counts in the bronchoalveolar lavage fluid (BALF). (**d**) Representative section and inflammatory scores of hematoxylin-eosin staining of lung sections. Scale bar, 50 μm. (**e**) Representative staining and percentage of periodic acid Schiff (PAS)-stained goblet cells per total epithelial cells in randomly selected bronchi. Scale bar, 50 μm. $n = 5$; data are representative of one of two (**a**) or three (**b–e**) independent experiments. Error bars show means ± s.d. *, OVA versus OVA and adjuvant; °, WT OVA and adjuvant versus *Irf3*$^{-/-}$ OVA and adjuvant; *,°$P < 0.05$, **,°°$P < 0.01$, ***$P < 0.001$.

airway challenge with OVA, we observed that *Irf3*$^{-/-}$ mice were protected from allergic airway inflammation (**Fig. 4c–e**), and that their BLN cells showed impaired proliferation and T_H2 cytokine secretion in response to OVA re-stimulation (**Supplementary Fig. 9a,b**). It is noteworthy that *Irf3*$^{-/-}$ mice, when compared with WT mice, had decreased serum OVA-specific IgE levels but similar OVA-specific IgG1 titers in this model (**Supplementary Fig. 9c,d**).

Previous studies in our laboratory indicated that *Irf3*$^{-/-}$ mice show normal boosting of T_H2 responses by Irf3-independent adjuvants[31]. Moreover, *Irf3*$^{-/-}$ T cells proliferate and secrete T_H2 cytokines normally in response to CD3 and CD28 stimulation (**Supplementary Fig. 10a,b**). *Irf3*$^{-/-}$ mice also develop humoral responses similar to those of WT mice when immunized with Freund's adjuvant (**Supplementary Fig. 11a–c**).

Taken together, these results indicate that *Irf3*$^{-/-}$ mice are impaired in their ability to boost T_H2 cell responses to alum immunization and to genomic DNA. They further suggest that Irf3-dependent T_H2 cell responses to alum may sustain tissue inflammation but do not affect IgG1 production. The T_H cells implicated in these Irf3-dependent responses would thus functionally correspond to canonical T_H2 cells[32]. In addition, T cell responses, although reduced, were not completely abrogated in *Irf3*$^{-/-}$ mice (**Fig. 4a,b** and **Supplementary Fig. 8a,b**). This suggests that Irf3-independent pathways also contribute to the adjuvant activity of alum on T cell responses, and that these Irf3-independent T cell responses primarily sustain B cell responses, including IgG1 production.

Alum-activated iDCs boost canonical T_H2 responses

The inability of *Irf3*$^{-/-}$ mice to produce normal T_H2 cell responses suggested the possibility of deficient antigen presentation to T cells. We thus studied the recruitment of dendritic cells and other innate immune cells to alum injection sites and their draining lymph nodes. Although the recruitment of immune cell populations at sites of alum injection did not differ significantly between WT and *Irf3*$^{-/-}$ mice (**Supplementary Fig. 12a,b**), there was a reduction in the numbers of inflammatory monocyte (iMono)-derived inflammatory DCs (iDCs) and, to a lesser extent, of conventional DCs (cDCs) in the draining lymph nodes of i.p. or i.m. OVA and alum–treated *Irf3*$^{-/-}$ mice, whereas numbers of plasmacytoid DCs (pDCs) were not reduced (**Fig. 5a** and **Supplementary Fig. 13a**). Similarly, i.p. or i.m. OVA and DNA treatment induced an Irf3-dependent recruitment of iDCs to the BLNs (**Fig. 5b** and **Supplementary Fig. 13b**). Adding further support to the idea that host DNA acts as a trigger of iDC recruitment upon alum immunization, we observed that the recruitment of iDCs to the BLNs of alum-treated mice strongly correlated with the percentage of cell death and DNA release (**Fig. 5c**), and that it was reduced after DNase I treatment (**Fig. 5d**).

Our observations suggested that Irf3 may be required for T_H2 cell and IgE responses through its role in the normal recruitment of iMonos, the precursors of iDCs[11,33,34], to the lymph nodes that drain alum injection sites. Supporting this hypothesis, we found that the transfer of iMonos isolated from OVA and alum–immunized WT mice to *Irf3*$^{-/-}$ mice treated with OVA and alum increased the proliferation of transferred CFSE-labeled OVA-specific CD4+ cells (**Fig. 5e**) and the differentiation of endogenous OVA-specific CD4+ T_H2 cells (**Supplementary Fig. 14a,b**). In addition, we found that transferring WT iMonos to OVA and alum–treated *Irf3*$^{-/-}$ mice increased T_H2-type cytokine production (**Fig. 5f**) and OVA-specific IgE titers (**Fig. 5g**), almost to the levels of OVA and alum–treated WT mice. In contrast, iMono transfer did not affect OVA-specific IgG1 titers (**Fig. 5h**). Notably, we observed that, although the transfer of iMonos from OVA and alum–treated mice was sufficient to induce robust T_H2 cell responses in the draining lymph nodes of naive recipient mice (**Supplementary Fig. 15a–d**), it did not induce any detectable IgG1 or IgE responses (data not shown).

These results therefore indicate that Irf3 is essential for the triggering of iDC recruitment by alum. They also suggest that these iDCs subsequently induce a canonical T_H2 response that is unable to

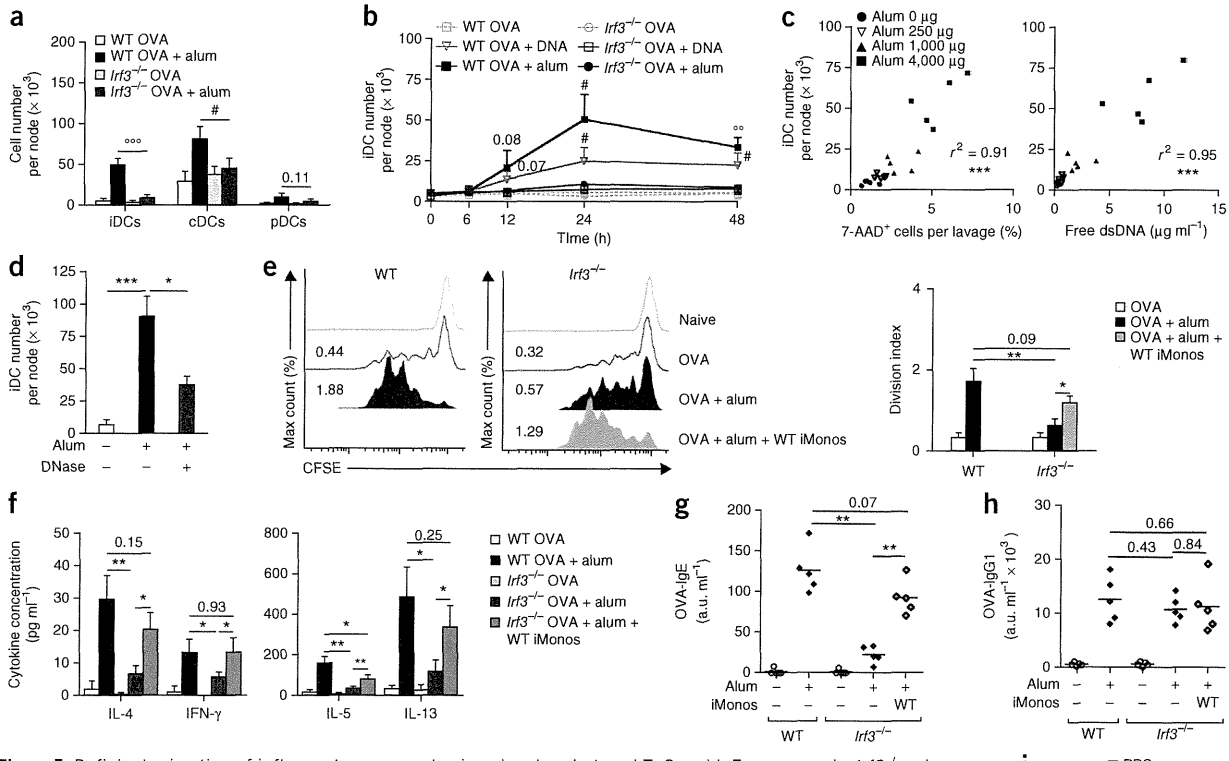

Figure 5 Deficient migration of inflammatory monocytes impairs alum-induced T_H2 and IgE responses in *Irf3*$^{-/-}$ mice. (**a**) Flow cytometric assessment of the numbers of iDCs, cDCs and pDCs in the BLNs of WT and *Irf3*$^{-/-}$ mice 24 h after i.p. injection of OVA or OVA and alum. (**b**) Recruitment of iDCs to the BLNs of WT and *Irf3*$^{-/-}$ mice treated i.p. with OVA, OVA and DNA, or OVA and alum. (**c**) Correlation between the percentage of cell death (assessed as in **Fig. 1c**), DNA release (assessed as in **Fig. 1a**), and the recruitment of iDCs to the BLN (assessed as in **b**, at 24 h) of WT mice treated with alum for 24 h. (**e**) Proliferation profile (left) and division index (right) of adoptively transferred OVA-specific CD4+ OT-II cells in the BLNs of *Irf3*$^{-/-}$ mice that received OVA and alum and an adoptive transfer of WT iMonos obtained from the peritoneal cavity of OVA and alum–treated WT mice. Inserted numbers indicate division index values. (**f**) Cytokine concentrations in the supernatant of OVA-stimulated BLN cells isolated from *Irf3*$^{-/-}$ mice that received OVA and alum and an adoptive transfer of WT iMonos obtained as in **e**. (**g**,**h**) Serum titers of OVA-specific IgE (**g**) and IgG1 (**h**) in *Irf3*$^{-/-}$ mice treated with OVA and alum, transferred with WT iMonos as in **e** on days 0 and 14, and then boosted with OVA on day 21. As controls, we used WT and *Irf3*$^{-/-}$ mice that received PBS with OVA alone or OVA and alum. (**i**) Numbers of CFSE+ iDCs in the BLNs of OVA and alum–treated WT mice that received CFSE-labeled WT or *Irf3*$^{-/-}$ iMonos 18 h earlier. Control mice received PBS alone. $n = 5$; data are representative of one of four (**a**,**c**), one of three (**f**–**i**) or one of two (**b**,**d**,**e**) independent experiments. Error bars show means ± s.d. #, WT OVA and adjuvant versus *Irf3*$^{-/-}$ OVA and adjuvant (**a**,**b**); *,°$P < 0.05$, **,°°$P < 0.01$, ***,°°°$P < 0.001$. a.u., arbitrary unit.

autonomously support humoral responses, but that has the ability to promote IgE responses from independently activated B cell responses.

Alum-induced IL-12p80 promotes iMono migration

Cross-transfer experiments suggested that *Irf3*$^{-/-}$ iMonos had a cell-intrinsic defect that rendered them unable to migrate to the lymph nodes after alum treatment (**Fig. 5i**). In cells isolated from sites of OVA and alum injection, the production of IFN-β1, a hallmark of Irf3 activation, was most prominent in iMonos, as compared with other peritoneal cells (**Supplementary Fig. 16**). We found that IFN-β1 production was abrogated in iMonos from *Irf3*$^{-/-}$ mice, suggesting that Irf3 indeed is activated in iMonos (**Supplementary Fig. 16**). As demonstrated by the use of *Irf9*$^{-/-}$ mice and mice lacking the gene encoding interferon α- and β- receptor 2 (*Ifnar2*$^{-/-}$ mice), type I and type III IFNs did not affect alum-induced iDC recruitment or humoral responses (data not shown).

Although Irf3 deficiency did not seem to affect the overall maturation state of iMonos (a process usually associated with the acquisition of migratory activity), we noticed that a higher proportion of *Irf3*$^{-/-}$ iMonos highly expressed CCR7, a chemokine receptor crucial for DC migration to the lymph nodes, compared with their WT counterparts (**Fig. 6a**). This suggested that *Irf3*$^{-/-}$ iMonos might be unable to respond to CCR7-activating signals, which would lead to their accumulation. Recent evidence indicates that iMono-derived DCs depend on signaling by homodimers of IL-12p40 (IL-12p80) for their ability to respond to CCR7-activating chemokines[35,36]. We found that alum induced the local production of IL-12p80 in WT mice, and that this production was reduced in *Irf3*$^{-/-}$ mice (**Fig. 6b**). We showed the importance of IL-12p80 expression in regulating iMono migration by treating *Irf3*$^{-/-}$ mice with recombinant IL-12p80, which restored migration of iDCs to the BLNs of alum-injected *Irf3*$^{-/-}$ mice, almost to the levels seen in WT mice (**Fig. 6c**). Moreover, neutralization of IL-12p80 by p40-specific neutralizing antibodies partially attenuated IgE responses and the recruitment of iDCs to the BLNs in OVA and alum–treated WT mice, whereas it did not affect IgG1 responses (**Fig. 6d–f**). Thus, these results suggest that alum-induced iDC activation relies on signaling by IL-12p80.

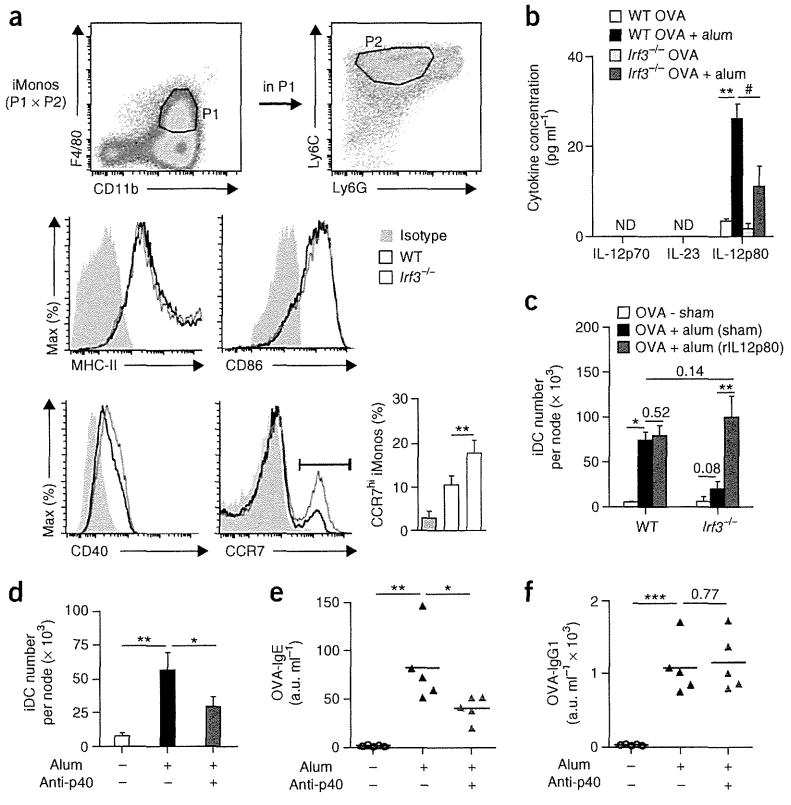

Figure 6 Alum-induced iMono migration depends on IL-12p40 homodimer signaling. (**a**) Gating strategy for iMonos and flow cytometric analysis of their surface expression of CCR7 and co-stimulatory molecules in OVA and alum–treated WT and *Irf3*$^{-/-}$ mice. Bottom right, percentage of CCR7^{hi} iMonos in OVA and alum–treated WT and *Irf3*$^{-/-}$ mice is indicated. (**b**) ELISA measurement of IL-12p70, IL-23 and IL-12p80 in the acellular phase of the peritoneal lavage fluid of WT and *Irf3*$^{-/-}$ mice treated overnight with OVA or with OVA and alum. #, WT OVA and alum versus *Irf3*$^{-/-}$ OVA and alum. (**c**,**d**) Recruitment of iDCs to the BLNs of WT and *Irf3*$^{-/-}$ mice treated with OVA and alum and recombinant IL-12p80 (rIL12p80) (**c**) or p40-specific neutralizing antibody (**d**). Control OVA- and OVA and alum–treated mice received PBS only. (**e**,**f**) Serum titers of OVA-specific IgE (**e**) and IgG1 (**f**) measured on day 17 in WT mice treated i.p. with OVA and alum and p40-specific neutralizing antibody, and then boosted with OVA i.p. 10 d later. $n = 5$; data are representative of one of three (**a**) or two (**b**–**f**) independent experiments. Error bars show means ± s.d. $^{*}P < 0.05$, $^{**}P < 0.01$, $^{***}P < 0.001$. a.u., arbitrary unit.

DISCUSSION

Extracellular host DNA has been recently recognized as a DAMP, and it seems to be involved in an increasing number of immune processes and diseases[16,19,37–39]. In this study, we show that host DNA released at sites of injection by dying cells can mediate the adjuvant effect of alum on adaptive responses. Our data thus support the idea that DAMPs have a key role in the adjuvant activity of alum and that, like any other efficient adjuvant[40,41], alum acts mainly by triggering innate immunity. In this regard, it should also be noted that uric acid, a major metabolite of nucleic acids and a potential DAMP when crystallized, has been suggested to have a role in iDC recruitment and T cell activation after alum immunization[11].

It has recently been proposed that alum immunization may induce functionally distinct T_H cell subsets comprising T follicular helper (T_{FH}) cells, which would be responsible for B cell help, and lymphoid and emigrant T_H cells, which would be responsible for other effector functions[42]. Another report suggested that IL-4–producing T_{FH} cells may be distinguished functionally from canonical T_H2 cells[32]. These IL-4–producing T_{FH} cells, also referred to as $T_{FH}2$ cells[43], would be endowed with high B cell helper activity and would promote IgG1 responses, but they would be poor inducers of classical T_H2 cell effector functions in peripheral tissues[32]. Canonical T_H2 cells, on the contrary, would be specialized in mediating T_H2 cell effector functions in peripheral tissues[32].

In line with these studies, our data allow us to propose a model in which the contribution of host DNA to the adjuvant activity of alum would comprise both an Irf3-independent and an Irf3-dependent component (**Supplementary Fig. 17**). In the Irf3-independent component of the response, host DNA induces IgG1 production through the promotion of T_H responses endowed with high B cell helper activity. These T_H cells would thus functionally relate to $T_{FH}2$ cells. In the Irf3-dependent component, iDCs activated by host DNA trigger T_H2 cell responses that mediate effector T_H2 cell functions in peripheral tissues but lack the ability to stimulate antibody production on their own. These T_H cells would thus functionally relate to canonical T_H2 cells. They would also promote IgE production from independently induced B cell responses. Future detailed phenotypic and functional characterization of these T_H cell subtypes should offer new perspectives on the mechanisms driving the production of specific antibody responses.

Our data suggest that alum-activated iDCs preferentially induce canonical T_H2 cell responses. In other settings, iMono-derived iDCs preferentially induce other types of T_H responses, such as T_H1 responses[44]. The functional specialization of iDCs upon alum immunization most probably originates from the T_H2 microenvironment that develops at alum injection sites[10]. In contrast with a previous report[11], we observed that impairment of iDC function does not affect IgG1 production. This disagreement probably comes from the fact that the general depletion of CD11c^{+} cells used to target iDCs in the previous study also depleted other CD11c^{+} APCs. Given the diversity of lymph node APCs[45] and the current lack of molecular tools for manipulating them specifically *in vivo*, the identification of the APC(s) responsible for initiating IgG1 responses will be a stimulating challenge for future research.

It is traditionally thought that IgG1 and IgE responses are sequentially boosted by a common IL-4–producing T_H cell response. Our data, however, support the idea that IgE and IgG1 responses are uncoupled and that they are regulated by functionally distinct T_H cell mechanisms. Understanding how alum-induced DNA release stimulates $T_{FH}2$-related T cell help for IgG1 production could thus have a promising influence on the design of new vaccine formulations devoid of canonical T_H2 cell and IgE bias. We foresee that this breakthrough might come from the identification of the DNA sensors triggered by alum.

In conclusion, we suggest that the DNA released by dying host cells is an important DAMP mediating the adjuvant activity of alum.

This knowledge may help in improving or developing current and experimental adjuvant formulations, which will be key to the success of future vaccination strategies.

METHODS

Methods and any associated references are available in the online version of the paper at http://www.nature.com/naturemedicine/.

Note: Supplementary information is available on the Nature Medicine website.

ACKNOWLEDGMENTS

The authors thank T. Taniguchi (University of Tokyo) and RIKEN BioResource Center for providing *Irf3*$^{-/-}$ and *Irf9*$^{-/-}$ mice, and V. Dixit (Genentech) for providing *Nlrp3*$^{-/-}$ and *Casp1*$^{-/-}$ mice. We also thank S. Ormenese and R. Stephaan of the Cell Imaging and Flow Cytometry Technological Platform of the Groupe Interdisciplinaire de Génoprotéomique Appliquée for help with fluorescent-activated cell sorting (FACS) analyses; M. Lebrun for help with confocal microscopy; P. Drion and G. Gaudray for animal management; F. Andris, S. Goriely and O. Leo for helpful discussions; and V. Conrath, L. Duwez, R. Fares, C. François, F. Olivier, J. Parisi, F. Perin and I. Sbai for excellent technical and secretarial assistance.

T.M., D.B., C.M. and C.S. are research fellows, and C.J.D. is a postdoctoral fellow of the Fonds National de la Recherche Scientifique (FRS-FNRS; Belgium). This work was supported by grants of the FRS-FNRS, the Belgian Fonds de la Recherche Scientifique Médicale and the Belgian Programme on Interuniversity Attraction Poles (IUAP; FEDIMMUNE, Belgian Science Policy). This work was also partly supported by the Knowledge Cluster Initiative (K.J.I.); a Grant-in-Aid for Scientific Research (K.J.I. and C.C.) of the Japanese Ministry of Education, Culture, Sports, Science and Technology (MEXT); and by the Core Research Evolutionary Science and Technology (CREST) program at the Japan Science and Technology Agency (K.J.I.).

AUTHOR CONTRIBUTIONS

T.M., K.J.I., F.B. and C.J.D. designed the experiments; C.C., K.J.I., F.B. and C.J.D. supervised the project; T.M. and D.B. made the initial observation; T.M. did most of the experiments and compiled the data; T.M., K.O. and K.K. did the experiments involving *Tbk1/Tnf* double-knockout mice, *Zbp1*$^{-/-}$, *Ifnar2*$^{-/-}$ and *Mavs*$^{-/-}$ mice; C.M. and C.S. did the FACS analyses; S.A. provided the *Tbk1/Tnf* double-knockout mice and *Zbp1*$^{-/-}$ mice; P.L., S.A., K.J.I. and F.B. secured funding; K.J.I. and F.B. provided feedback on the manuscript; and C.J.D. wrote the manuscript.

COMPETING FINANCIAL INTERESTS

The authors declare no competing financial interests.

Published online at http://www.nature.com/naturemedicine/.
Reprints and permissions information is available online at http://www.nature.com/reprints/index.html.

1. Glenny, A.T., Pope, C.G., Waddington, H. & Wallace, U. Immunological Notes: XVII–XXIV. *J. Pathol. Bacteriol.* **29**, 31–40 (1926).
2. Mannhalter, J.W., Neychev, H.O., Zlabinger, G.J., Ahmad, R. & Eibl, M.M. Modulation of the human immune response by the non-toxic and non-pyrogenic adjuvant aluminium hydroxide: effect on antigen uptake and antigen presentation. *Clin. Exp. Immunol.* **61**, 143–151 (1985).
3. Li, H., Nookala, S. & Re, F. Aluminum hydroxide adjuvants activate Caspase-1 and induce IL-1β and IL-18 release. *J. Immunol.* **178**, 5271–5276 (2007).
4. Hornung, V. *et al.* Silica crystals and aluminum salts activate the NALP3 inflammasome through phagosomal destabilization. *Nat. Immunol.* **9**, 847–856 (2008).
5. Eisenbarth, S.C., Colegio, O.R., O'Connor, W., Sutterwala, F.S. & Flavell, R.A. Crucial role for the Nalp3 inflammasome in the immunostimulatory properties of aluminium adjuvants. *Nature* **453**, 1122–1126 (2008).
6. Franchi, L. & Nunez, G. The Nlrp3 inflammasome is critical for aluminium hydroxide-mediated IL-1β; secretion but dispensable for adjuvant activity. *Eur. J. Immunol.* **38**, 2085–2089 (2008).
7. Kool, M. *et al.* Cutting Edge: alum adjuvant stimulates inflammatory dendritic cells through activation of the NALP3 inflammasome. *J. Immunol.* **181**, 3755–3759 (2008).
8. Li, H., Willingham, S.B., Ting, J.P.Y. & Re, F. Cutting Edge: Inflammasome activation by alum and alum's adjuvant effect are mediated by NLRP3. *J. Immunol.* **181**, 17–21 (2008).
9. Spreafico, R., Ricciardi-Castagnoli, P. & Mortellaro, A. The controversial relationship between NLRP3, alum, danger signals and the next-generation adjuvants. *Eur. J. Immunol.* **40**, 638–642 (2010).
10. McKee, A.S. *et al.* Alum induces innate immune responses through macrophage and mast cell sensors, but these sensors are not required for alum to act as an adjuvant for specific immunity. *J. Immunol.* **183**, 4403–4414 (2009).
11. Kool, M. *et al.* Alum adjuvant boosts adaptive immunity by inducing uric acid and activating inflammatory dendritic cells. *J. Exp. Med.* **205**, 869–882 (2008).
12. Goto, N. *et al.* Local tissue irritating effects and adjuvant activities of calcium phosphate and aluminium hydroxide with different physical properties. *Vaccine* **15**, 1364–1371 (1997).
13. Kono, H. & Rock, K.L. How dying cells alert the immune system to danger. *Nat. Rev. Immunol.* **8**, 279–289 (2008).
14. Chen, G.Y. & Nunez, G. Sterile inflammation: sensing and reacting to damage. *Nat. Rev. Immunol.* **10**, 826–837 (2010).
15. Ishii, K.J. *et al.* Genomic DNA released by dying cells induces the maturation of APCs. *J. Immunol.* **167**, 2602–2607 (2001).
16. Takeshita, F. & Ishii, K.J. Intracellular DNA sensors in immunity. *Curr. Opin. Immunol.* **20**, 383–388 (2008).
17. Takeuchi, O. & Akira, S. Pattern recognition receptors and inflammation. *Cell* **140**, 805–820 (2010).
18. Lande, R. *et al.* Plasmacytoid dendritic cells sense self-DNA coupled with antimicrobial peptide. *Nature* **449**, 564–569 (2007).
19. Imaeda, A.B. *et al.* Acetaminophen-induced hepatotoxicity in mice is dependent on Tlr9 and the Nalp3 inflammasome. *J. Clin. Invest.* **119**, 305–314 (2009).
20. Takaoka, A. *et al.* DAI (DLM-1/ZBP1) is a cytosolic DNA sensor and an activator of innate immune response. *Nature* **448**, 501–505 (2007).
21. Muruve, D.A. *et al.* The inflammasome recognizes cytosolic microbial and host DNA and triggers an innate immune response. *Nature* **452**, 103–107 (2008).
22. Chiu, Y.-H., MacMillan, J.B. & Chen, Z.J. RNA Polymerase III detects cytosolic DNA and induces type I Interferons through the RIG-I pathway. *Cell* **138**, 576–591 (2009).
23. Fernandes-Alnemri, T., Yu, J.-W., Datta, P., Wu, J. & Alnemri, E.S. AIM2 activates the inflammasome and cell death in response to cytoplasmic DNA. *Nature* **458**, 509–513 (2009).
24. Hornung, V. *et al.* AIM2 recognizes cytosolic dsDNA and forms a caspase-1-activating inflammasome with ASC. *Nature* **458**, 514–518 (2009).
25. Ishikawa, H., Ma, Z. & Barber, G.N. STING regulates intracellular DNA-mediated, type I interferon-dependent innate immunity. *Nature* **461**, 788–792 (2009).
26. Yanai, H. *et al.* HMGB proteins function as universal sentinels for nucleic-acid-mediated innate immune responses. *Nature* **462**, 99–103 (2009).
27. Yang, P. *et al.* The cytosolic nucleic acid sensor LRRFIP1 mediates the production of type I interferon via a β-catenin-dependent pathway. *Nat. Immunol.* **11**, 487–494 (2010).
28. Ishii, K.J. *et al.* A Toll-like receptor-independent antiviral response induced by double-stranded B-form DNA. *Nat. Immunol.* **7**, 40–48 (2006).
29. Bonnard, M. *et al.* Deficiency of T2K leads to apoptotic liver degeneration and impaired NF-κB-dependent gene transcription. *EMBO J.* **19**, 4976–4985 (2000).
30. Ishii, K.J. *et al.* TANK-binding kinase-1 delineates innate and adaptive immune responses to DNA vaccines. *Nature* **451**, 725–729 (2008).
31. Marichal, T. *et al.* Interferon response factor 3 is essential for house dust mite-induced airway allergy. *J. Allergy Clin. Immunol.* **126**, 836–844 (2010).
32. Reinhardt, R.L., Liang, H.-E. & Locksley, R.M. Cytokine-secreting follicular T cells shape the antibody repertoire. *Nat. Immunol.* **10**, 385–393 (2009).
33. Naik, S.H. *et al.* Intrasplenic steady-state dendritic cell precursors that are distinct from monocytes. *Nat. Immunol.* **7**, 663–671 (2006).
34. Shortman, K. & Naik, S.H. Steady-state and inflammatory dendritic-cell development. *Nat. Rev. Immunol.* **7**, 19–30 (2007).
35. Khader, S.A. *et al.* Interleukin 12p40 is required for dendritic cell migration and T cell priming after Mycobacterium tuberculosis infection. *J. Exp. Med.* **203**, 1805–1815 (2006).
36. Robinson, R.T. *et al. Yersinia pestis* evades TLR4-dependent induction of IL-12(p40)2 by dendritic cells and subsequent cell migration. *J. Immunol.* **181**, 5560–5567 (2008).
37. Yasutomo, K. *et al.* Mutation of DNASE1 in people with systemic lupus erythematosus. *Nat. Genet.* **28**, 313–314 (2001).
38. Yoshida, H., Okabe, Y., Kawane, K., Fukuyama, H. & Nagata, S. Lethal anemia caused by interferon-beta produced in mouse embryos carrying undigested DNA. *Nat. Immunol.* **6**, 49–56 (2005).
39. Kawane, K. *et al.* Chronic polyarthritis caused by mammalian DNA that escapes from degradation in macrophages. *Nature* **443**, 998–1002 (2006).
40. Pulendran, B. & Ahmed, R. Translating Innate Immunity into Immunological Memory: Implications for Vaccine Development. *Cell* **124**, 849–863 (2006).
41. Coffman, R.L., Sher, A. & Seder, R.A. Vaccine adjuvants: putting innate immunity to work. *Immunity* **33**, 492–503 (2010).
42. Fazilleau, N., McHeyzer-Williams, L.J., Rosen, H. & McHeyzer-Williams, M.G. The function of follicular helper T cells is regulated by the strength of T cell antigen receptor binding. *Nat. Immunol.* **10**, 375–384 (2009).
43. Fazilleau, N., Mark, L., McHeyzer-Williams, L.J. & McHeyzer-Williams, M.G. Follicular helper T cells: lineage and location. *Immunity* **30**, 324–335 (2009).
44. Nakano, H. *et al.* Blood-derived inflammatory dendritic cells in lymph nodes stimulate acute T helper type 1 immune responses. *Nat. Immunol.* **10**, 394–402 (2009).
45. Mohr, E. *et al.* Dendritic cells and monocyte/macrophages that create the IL-6/APRIL-rich lymph node microenvironments where plasmablasts mature. *J. Immunol.* **182**, 2113–2123 (2009).

ONLINE METHODS

Mice. *Tbk1/Tnf* DKO, *Tlr9*$^{-/-}$ and *Zbp1*$^{-/-}$ mice have been described elsewhere[28,46,47]. We purchased *Irf3*$^{-/-}$ (ref. 48) and *Irf9*$^{-/-}$ mice[49] from RIKEN BioResource Center. *Nlrp3*$^{-/-}$ and *Casp1*$^{-/-}$ mice[50,51] were a kind gift of V. Dixit (Genentech). *Ifnar2*$^{-/-}$ and *Mavs*$^{-/-}$ mice were obtained as described previously[30]. OVA-specific, MHC II–restricted, T cell receptor–transgenic OT-II (H-2b; C57BL/6 background) mice were obtained from The Jackson Laboratory. All transgenic mice except *Tbk1/Tnf* double-knockout and *Zbp1*$^{-/-}$ mice were backcrossed, in total, for 10 to 16 generations onto a C57Bl/6 background. *Tbk1/Tnf* double-knockout and *Zbp1*$^{-/-}$ mice were on a 129/Ola X C57Bl/6 background. *Tbk1*$^{+/-}$/*Tnf*$^{-/-}$ littermates were used as control for *Tbk1/Tnf* DKO mice. All mice were bred and housed in institution-specific pathogen-free facilities. Age-paired groups of females were used at 8–12 weeks of age. All experimental procedures and protocols were approved by the Institutional Animal Care and Use Committees of the University of Liège and of the Research Institute for Microbial Diseases, Osaka University, Japan.

Immunizations. Endotoxin-free (endotoxin <1 EU mg^{-1}) OVA was from Hyglos. Unless otherwise indicated, we immunized mice i.p. or i.m. with 10 μg of OVA alone or adsorbed on 4 mg of Imject Alum (OVA and alum; Pierce Biochemicals). For immunizations with genomic DNA, we purified genomic DNA from mouse tissue using High Pure PCR Template Preparation kits (Roche), and, unless otherwise indicated, we immunized mice with 10 μg of OVA mixed with 8 μg of DNA (OVA and DNA). The endotoxin content of the DNA preparations, as measured by Hyglos using the Limulus Amoebocyte Lysate assay, was always <1 EU mg^{-1}. Unless otherwise indicated, we immunized mice i.p. or i.m. on days 0 and 14 with 10 μg of OVA alone, of OVA and DNA or of OVA and alum, and then boosted them i.p. on day 21 with 20 μg of OVA. Alternatively, we replaced OVA with HSA (Sigma), and alum by Alhydrogel (Sigma).

***In vivo* DNase I treatment.** We injected mice i.p. with 2,000 IU of DNase I (Roche) in 100 μl of HBSS (Lonza) 3 and 18 h after immunization.

Measurement of antigen-specific antibody titers. For OVA- and HSA-specific IgG1 and OVA-specific IgM and IgG2c detection, we incubated diluted sera from immunized mice on ELISA plates coated with antigen at 100 μg ml^{-1}. We detected bound IgG1, IgM and IgG2c using horseradish peroxidase (HRP)-conjugated mouse IgG1-, IgM- and IgG2c-specific antibodies (Southern Biotechnology) followed by incubation with tetramethyl benzidine and measurement by spectrophotometry. For OVA- and HSA-specific IgE detection, we incubated diluted sera on ELISA plates coated with mouse IgE-specific antibodies (BD Biosciences) at 2 μg ml^{-1}. We detected bound IgE using biotinylated antigen followed by streptavidin peroxidase (Zymed) incubation. We calculated antibody titers by plotting the serum dilution that gave half-maximal signal. When no signal was detected, we assigned a titer of 2.

Antibodies. A detailed description of the antibodies used in this study is available in the **Supplementary Methods**.

Assessment of OVA-specific T cell activation. We assessed the proliferation of transferred CFSE-labeled OT-II cells, as described previously[52], 3 d after immunization. We assessed proliferation and IL-4 expression of endogenous OVA-specific CD4$^+$ cells as described previously[31], except that we cultured cells for 5 d with or without OVA (OVA grade V, Sigma; 50 μg ml^{-1}).

Flow cytometry and cell sorting. We incubated single cell suspensions with 2.4G2 Fc-receptor antibodies to reduce nonspecific binding before staining. We carried out staining reactions at 4 °C. We did flow cytometry on a FACScanto II instrument (BD Biosciences) and analyzed results using FlowJo software (Tree Star). We used a FACSAria instrument (BD Biosciences) for sorting F4/80^{int} CD11b$^+$Ly6C$^+$Ly6G$^-$ iMonos.

IL-12p40 homodimer ELISA, complementation and neutralization experiments. We measured IL-12p40 homodimer concentrations by ELISA as previously described[53]. Briefly, we used mouse recombinant IL-12p80 (Biolegend) as a standard. We used the standards for mouse IL-12p40, IL-12p70 and IL-23 (R&D Systems) to test the specificity of the ELISA. For complementation and neutralization experiments, we immunized mice with OVA and alum and, 6 and 18 h later, treated them with rIL-12p80 (1 μg in 100 μl of PBS) or low endotoxin azide-free–purified IL-12p40-specific antibodies (Biolegend) (500 μg in 100 μl of PBS), respectively.

Statistical analysis. Data are presented as means ± s.d. We estimated the differences between mean values by using two-tailed pairwise Student's *t* tests after Anderson-Darling tests for assessment of normality of the data distributions. We calculated correlation coefficients using Pearson's two-tailed tests after assessment of data distribution normality. In all figures, we use asterisk (*) and degree (°) symbols to indicate significant differences observed when comparing indicated groups (*,° $P < 0.05$; **,°° $P < 0.01$; and ***,°°° $P < 0.001$).

Additional methods. Detailed methodology is described in the **Supplementary Methods**.

46. Hemmi, H. *et al.* A Toll-like receptor recognizes bacterial DNA. *Nature* **408**, 740–745 (2000).
47. Hemmi, H. *et al.* The roles of two IκB kinase–related kinases in lipopolysaccharide and double stranded RNA signaling and viral infection. *J. Exp. Med.* **199**, 1641–1650 (2004).
48. Sato, M. *et al.* Distinct and essential roles of transcription factors IRF-3 and IRF-7 in response to viruses for IFN-α/β gene induction. *Immunity* **13**, 539–548 (2000).
49. Kimura, T. *et al.* Essential and non-redundant roles of p48 (ISGF3 gamma) and IRF-1 in both type I and type II interferon responses, as revealed by gene targeting studies. *Genes Cells* **1**, 115–124 (1996).
50. Mariathasan, S. *et al.* Differential activation of the inflammasome by caspase-1 adaptors ASC and Ipaf. *Nature* **430**, 213–218 (2004).
51. Mariathasan, S. *et al.* Cryopyrin activates the inflammasome in response to toxins and ATP. *Nature* **440**, 228–232 (2006).
52. Bedoret, D. *et al.* Lung interstitial macrophages alter dendritic cell functions to prevent airway allergy in mice. *J. Clin. Invest.* **119**, 3723–3738 (2009).
53. Nigg, A.P. *et al.* Dendritic cell-derived IL-12p40 homodimer contributes to susceptibility in cutaneous leishmaniasis in BALB/c mice. *J. Immunol.* **178**, 7251–7258 (2007).

doi:10.1038/nm.2403

DNA released from dying host cells mediates aluminum adjuvant activity

Thomas Marichal[1], Keiichi Ohata[2], Denis Bedoret[1], Claire Mesnil[1], Catherine Sabatel[1], Kouji Kobiyama[2,3], Pierre Lekeux[1], Cevayir Coban[2], Shizuo Akira[2], Ken J. Ishii[2,3,4], Fabrice Bureau[1,4], Christophe J. Desmet[1,4].

[1]Laboratory of Cellular and Molecular Physiology, GIGA-Research and Faculty of Veterinary Medicine, B34, University of Liege, 1 Avenue de l'Hopital, B4000 Liège, Belgium
[2]WPI Immunology Frontier Research Center, Osaka University, 3-1 Yamadaoka, Suita, 565-0871 Osaka, Japan
[3]Laboratory of Adjuvant Innovation, National Institute of Biomedical Innovation, 7-6-8 Asagi Saito Ibaraki-City Osaka, Japan
[4]These authors contributed equally to this work.

Correspondence should be addressed to C.J.D. (christophe.desmet@ulg.ac.be), F.B. (fabrice.bureau@ulg.ac.be) or K.J.I. (kenishii@biken.osaka-u.ac.jp).

Supplementary figures and legends 1-17

Supplementary methods

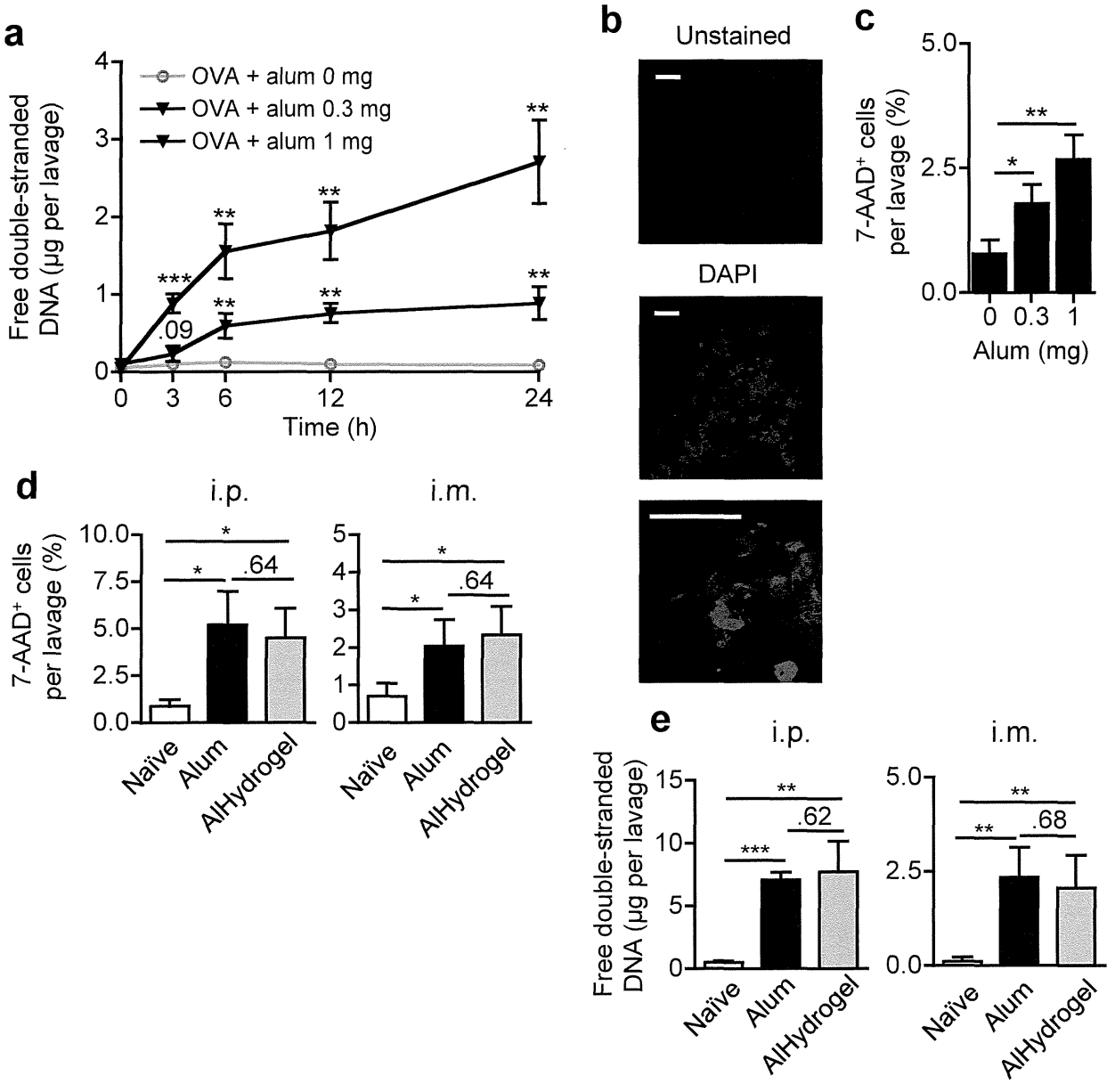

Supplementary Figure 1 Alum and AlHydrogel induce cell death and release of host DNA at sites of injection. (**a**) Concentration of free double-stranded (ds)DNA in the acellular fraction of the muscle lavage fluid of mice treated i.m. with increasing doses of alum, measured through time using quantitative fluorescent double-stranded DNA stain. (**b**) Extracellular DNA deposition in alum macroscopic i.m. depots stained with 4',6-diamidino-2-phenylindole (DAPI) (scale bar: 25 µm). (**c**) Cell death rate in the peritoneal lavage fluid of mice treated i.m. with increasing doses of alum, assessed by staining with 7-aminoactinomycin D (7-AAD) and flow cytometry. (**d,e**) Comparison of cell death rate (**d**) and dsDNA release (**e**) at i.p. and i.m. injection sites between alum- and AlHydrogel-treated mice. *n*=5 (**a,c-e**). Data are representative of one of three independent experiments.

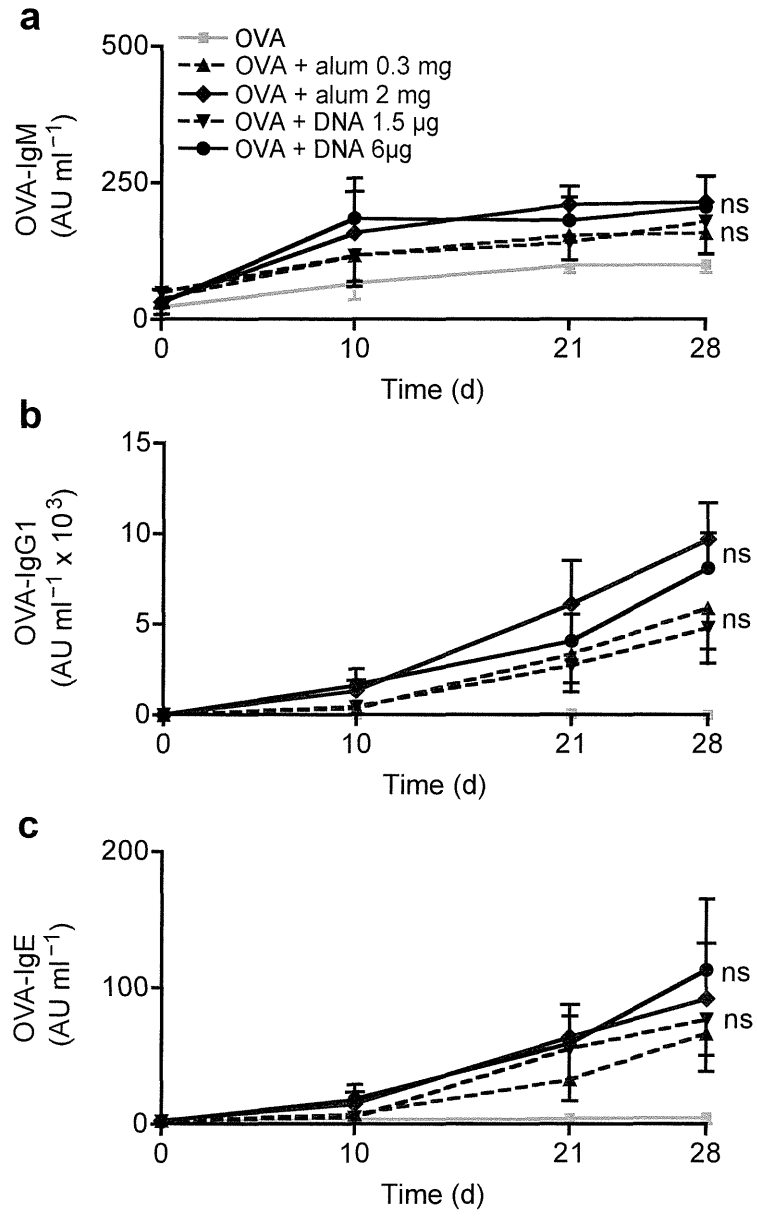

Supplementary Figure 2 Alum and host DNA injected i.m. potentiates type 2 humoral responses.(**a**) Serum titers of OVA-specific IgM, (**b**) IgG1 and (**c**) IgE measured on indicated days in mice immunized i.m. with OVA alone, OVA and alum, or OVA and DNA on days 0 and 14, and boosted with OVA on day 21. *n*=5. Data are representative of one of two experiments. (AU, arbitrary unit).

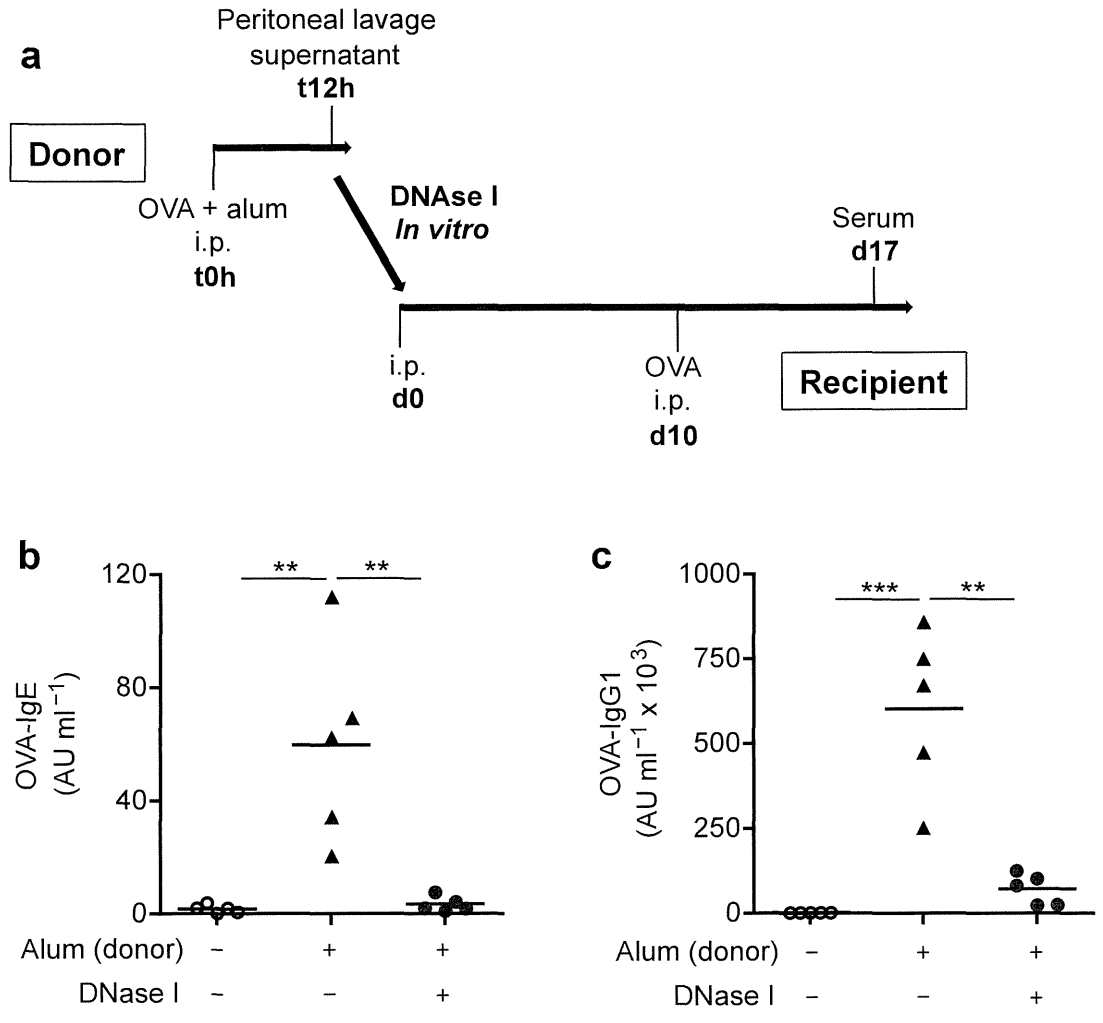

Supplementary Figure 3 DNA released upon alum treatment is necessary and sufficient to boost humoral responses. (**a**) Experimental outline. *In vitro*, we mock-treated or submitted to DNase I treatment the acellular fraction of peritoneal lavage fluid from OVA- or OVA and alum-treated mice, before transferring it to naïve recipient mice with 10µg OVA. We boosted recipient mice i.p. with OVA 10 d later. (**a,b**) ELISA measurement of OVA-specific IgE (**b**) and IgG1 (**c**) serum titers 7 d later. *n*=5. Data are representative of one of four independent experiments. (AU, arbitrary unit).

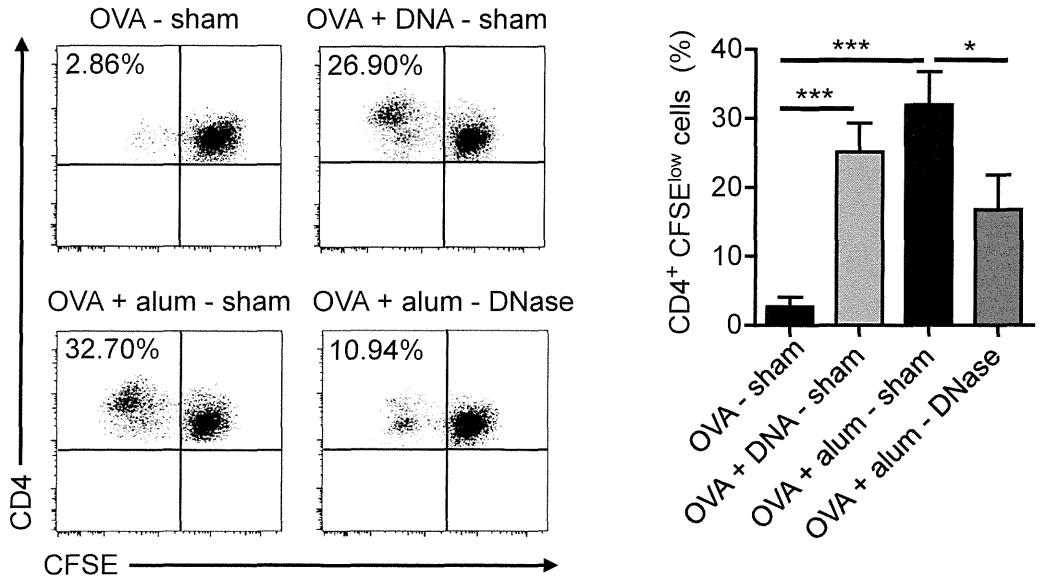

Supplementary Figure 4 Host DNA released by alum cytotoxicity mediates alum adjuvant activity on endogenous T cell responses. We treated mice i.p. with OVA, OVA and DNA, OVA and alum or OVA and alum followed by DNase I treatment. Five days later, we isolated bronchial lymph node (BLN) cells, labeled them with CFSE and restimulated them *in vitro* with OVA for 5 days. Cell viability remained high following carboxyfluorescein succinimidyl ester (CFSE) labeling (data not shown). We estimated the proliferation of OVA-specific CD4+ T cells by measuring the percentage of $CFSE^{low}$ $CD4^+$ T cells by flow cytometry (inserts indicate the percentage of $CFSE^{low}$ $CD4^+$ T cells). *n*=5. Data are representative of one of two independent experiments.

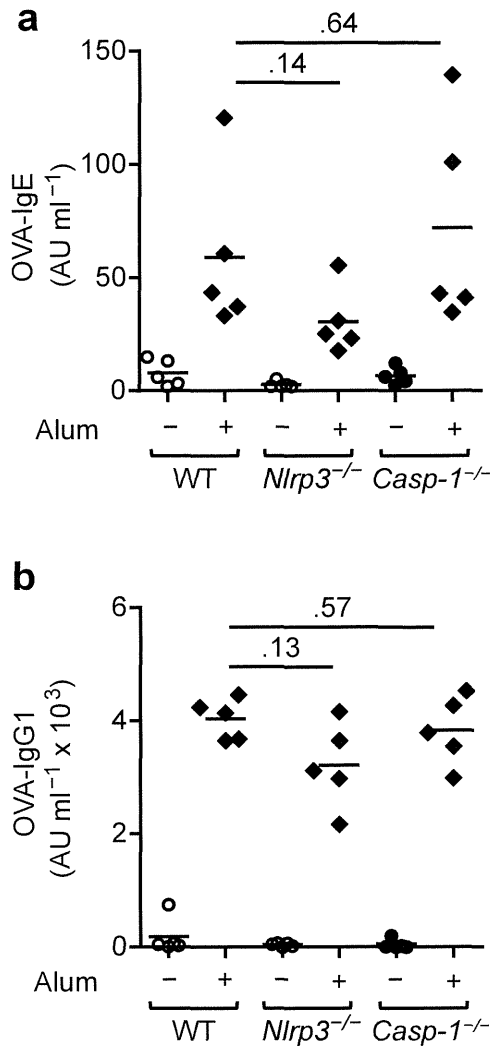

Supplementary Figure 5 *Nlrp3* or *Casp1* deficiency does not significantly impact on the adjuvant activity of alum on humoral responses. Serum OVA-specific IgE (**a**) and IgG1 (**b**) serum antibody titers measured on day 28 in WT, *Nlrp3*$^{-/-}$ and *Casp1*$^{-/-}$ mice immunized i.m. with OVA or OVA and 0.3 mg alum on days 0 and 14 and boosted with OVA on day 21. *n*=5. Data are representative of one of two independent experiments. (AU, arbitrary unit).

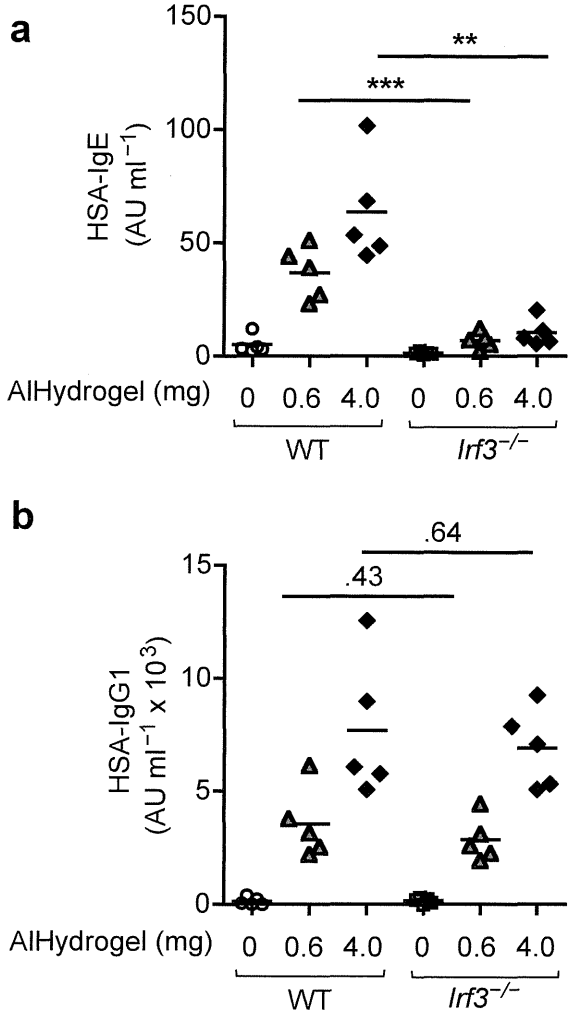

Supplementary Figure 6 The adjuvant activity of alum on antigen-specific IgE responses requires Irf3 independently of alum type and antigen. Serum HSA-specific IgE (**a**) and IgG1 (**b**) antibody titers measured on day 28 in *Irf3*$^{-/-}$ mice immunized i.p. with HSA or HSA combined with the indicated doses of AlHydrogel on days 0 and 14 and boosted with HSA i.p. on day 21. *n*=5. Data are representative of one of two independent experiments. (AU, arbitrary unit).

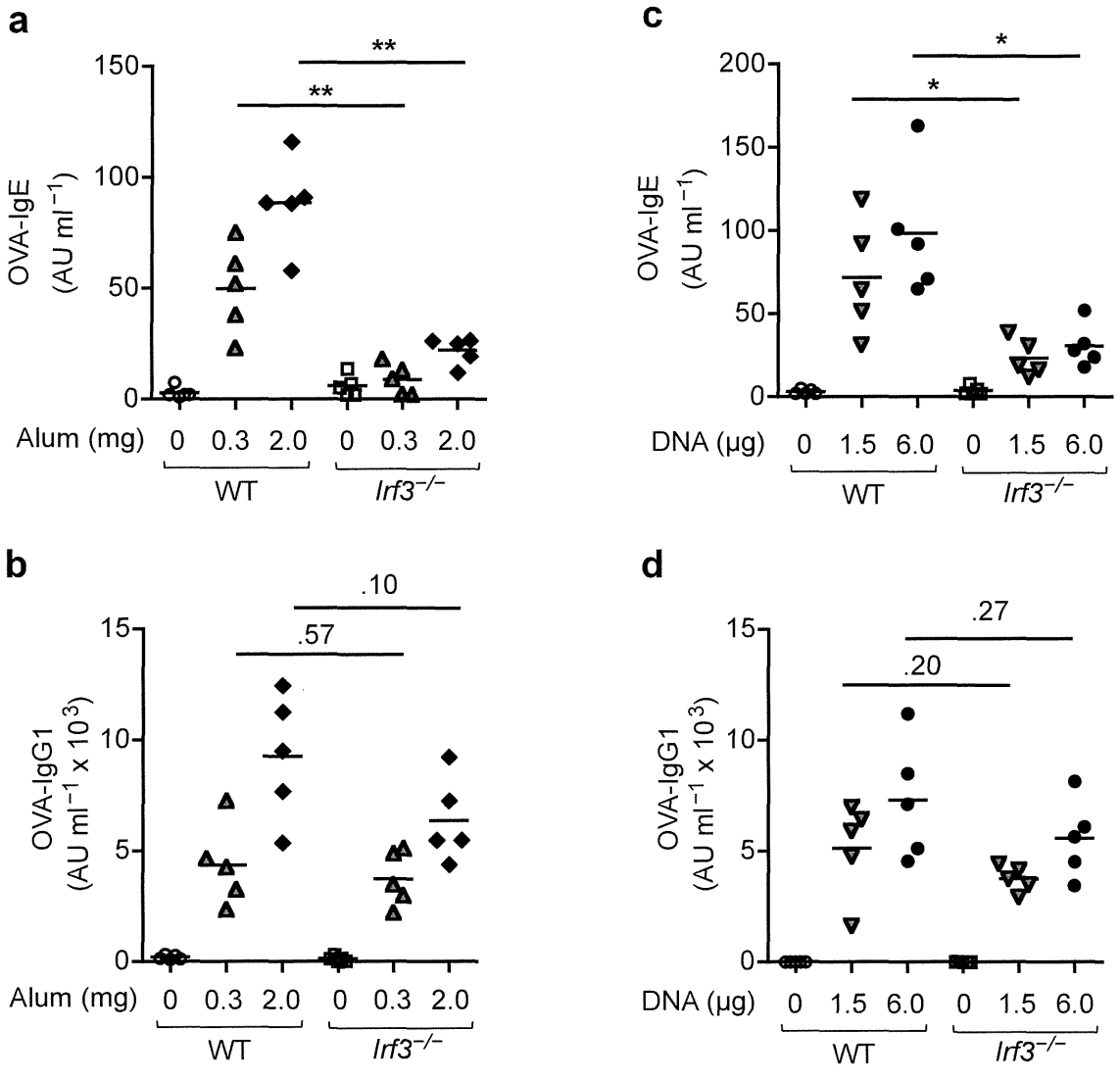

Supplementary Figure 7 The adjuvant activity of alum and host DNA on antigen-specific IgE responses requires Irf3 independently of the site of injection. Serum OVA-specific IgE (**a, c**) and IgG1 (**b, d**) antibody titers measured on day 28 in WT and *Irf3*$^{-/-}$ mice immunized i.m. with OVA or OVA combined with the indicated doses of alum or DNA on days 0 and 14 and boosted with OVA on day 21. *n*=5. Data are representative of one of two independent experiments. (AU, arbitrary unit).

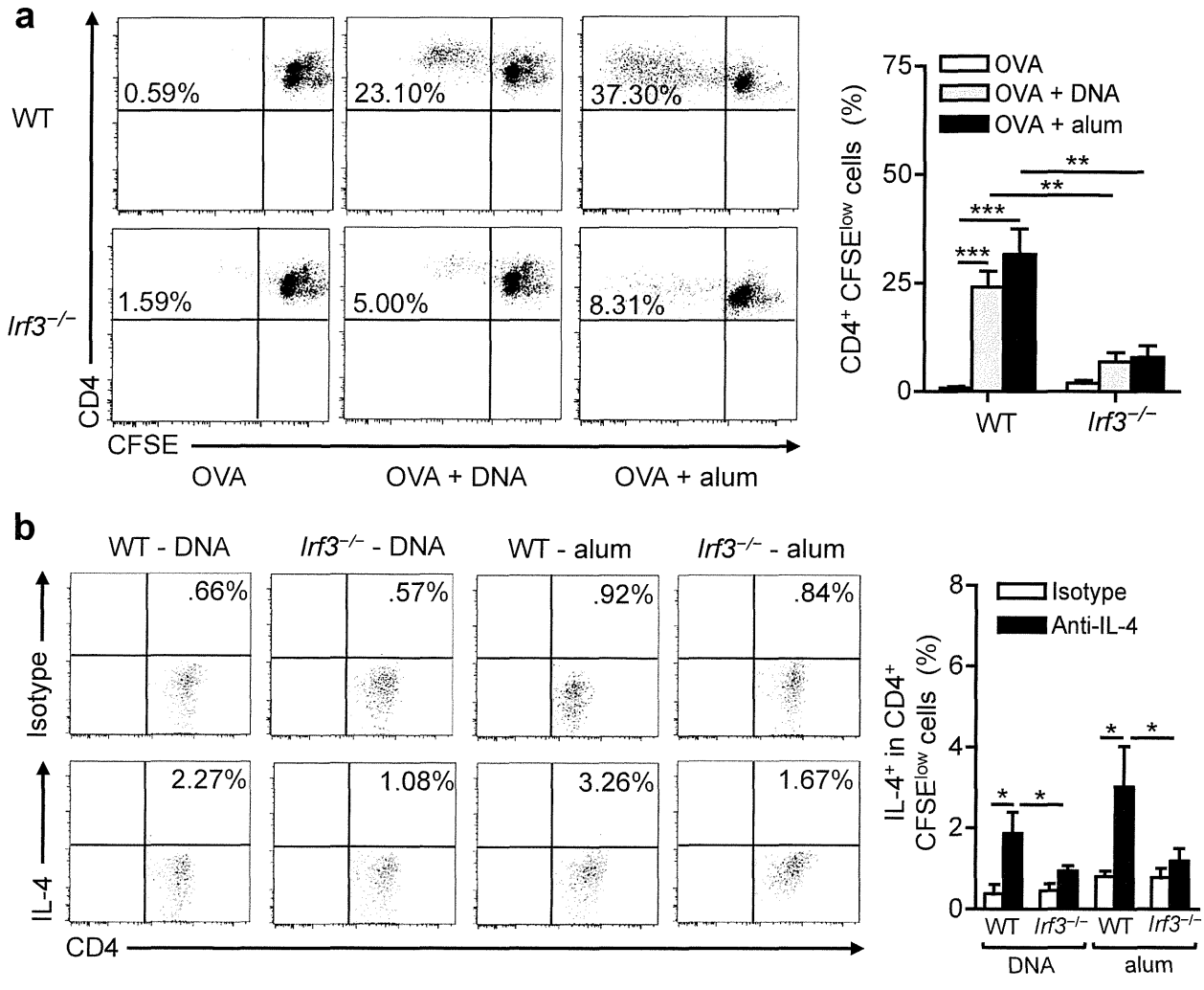

Supplementary Figure 8 Irf3 is essential for the boosting of type 2 T cell responses by alum and genomic DNA. We treated WT and *Irf3*$^{-/-}$ mice i.p. with OVA, OVA and DNA or OVA and alum. Five days later, we isolated BLN cells, labeled them with CFSE and restimulated them *in vitro* with OVA for 5 days. Cell viability remained high following carboxyfluorescein succinimidyl ester (CFSE) labeling and was not different between WT and *Irf3*$^{-/-}$ cells (data not shown). (**a**) Proliferation of OVA-specific CD4+ T cells estimated by measuring the percentage of CFSE^{low} CD4^{+} T cells by flow cytometry (inserts indicate the percentage of CFSE^{low} CD4^{+} T cells). (**b**) Percentages of IL4^{+} cells among CD4^{+} CFSE^{low} cells assessed by intracellular staining and flow cytometry (inserts indicate the percentage of IL4^{+} CFSE^{low} CD4^{+} T cells). *n*=5. Data are representative of one of three independent experiments.

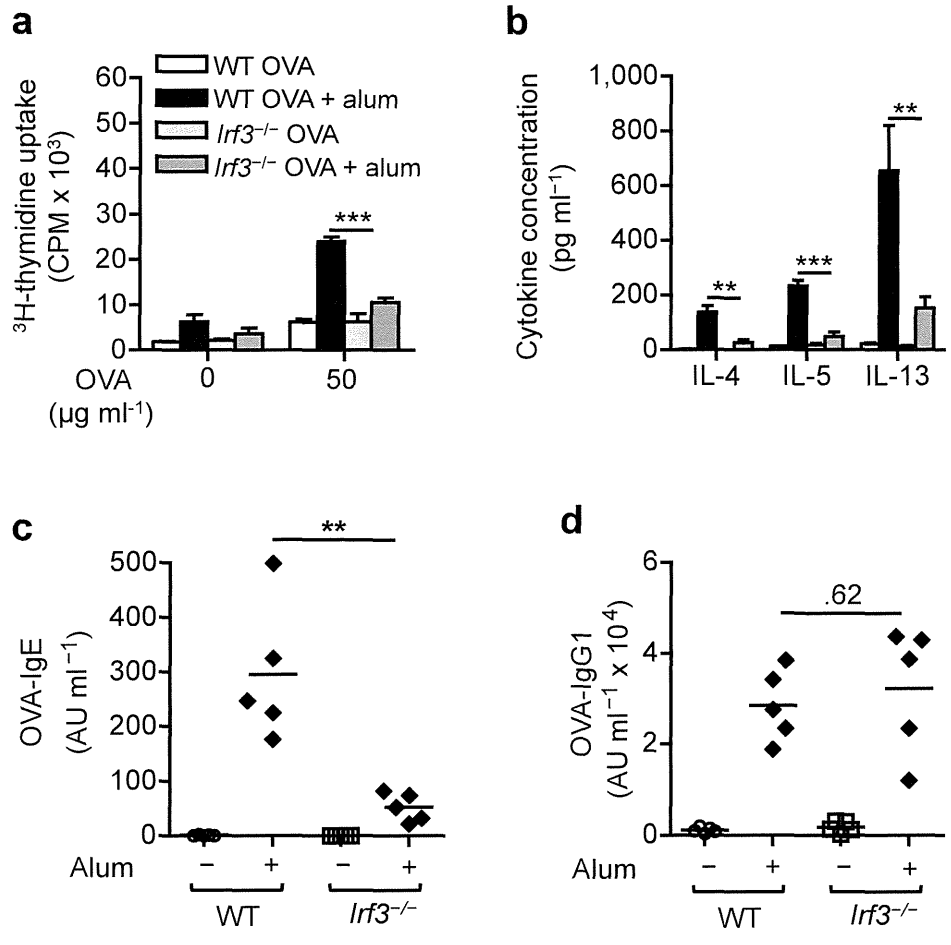

Supplementary Figure 9 Irf3 is essential for the boosting of 'canonical' Th2 cell differentiation and IgE responses in an alum-immunization-based asthma model. We challenged OVA- and OVA and alum-sensitized WT and *Irf3*$^{-/-}$ mice with aerosolized OVA and analyzed for type 2 T cell and humoral responses. (**a**) BLN cell proliferation in response to 3 days *in vitro* OVA stimulation assessed by the measurement of ^{3}H-thymidine uptake. (**b**) ELISA measurement of IL-4, IL-5 and IL-13 concentrations in culture supernatants of OVA-stimulated BLN cells. Serum OVA-specific IgE (**c**) and IgG1 (**d**) titers. *n*=5. Data are representative of one of three independent experiments. (CPM, counts per minute).

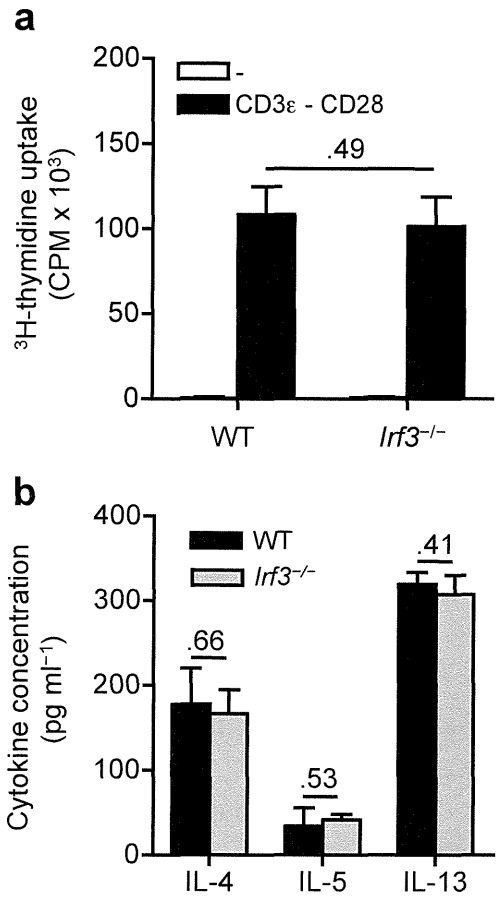

Supplementary Figure 10 WT and *Irf3*$^{-/-}$ T lymphocytes have similar potential for proliferation and Th2 cytokine secretion. (**a**) Proliferation assessed by measuring ^{3}H-thymidine incorporation during the last 16 hours of a 2-day culture of T cells (2 10^5 cells, >95% purity) purified from the BLNs of naïve WT and *Irf3*$^{-/-}$ mice and cultured with CD28-specific antibodies into plates coated with CD3-specific antibodies. We cultured controls in uncoated wells without CD28-specific antibodies. (**b**) ELISA measurement of IL-4, IL-5, IL-13 in the supernatant of the cells in a. *n*=5 . Data are representative of one of three independent experiments. (CPM, counts per minute)

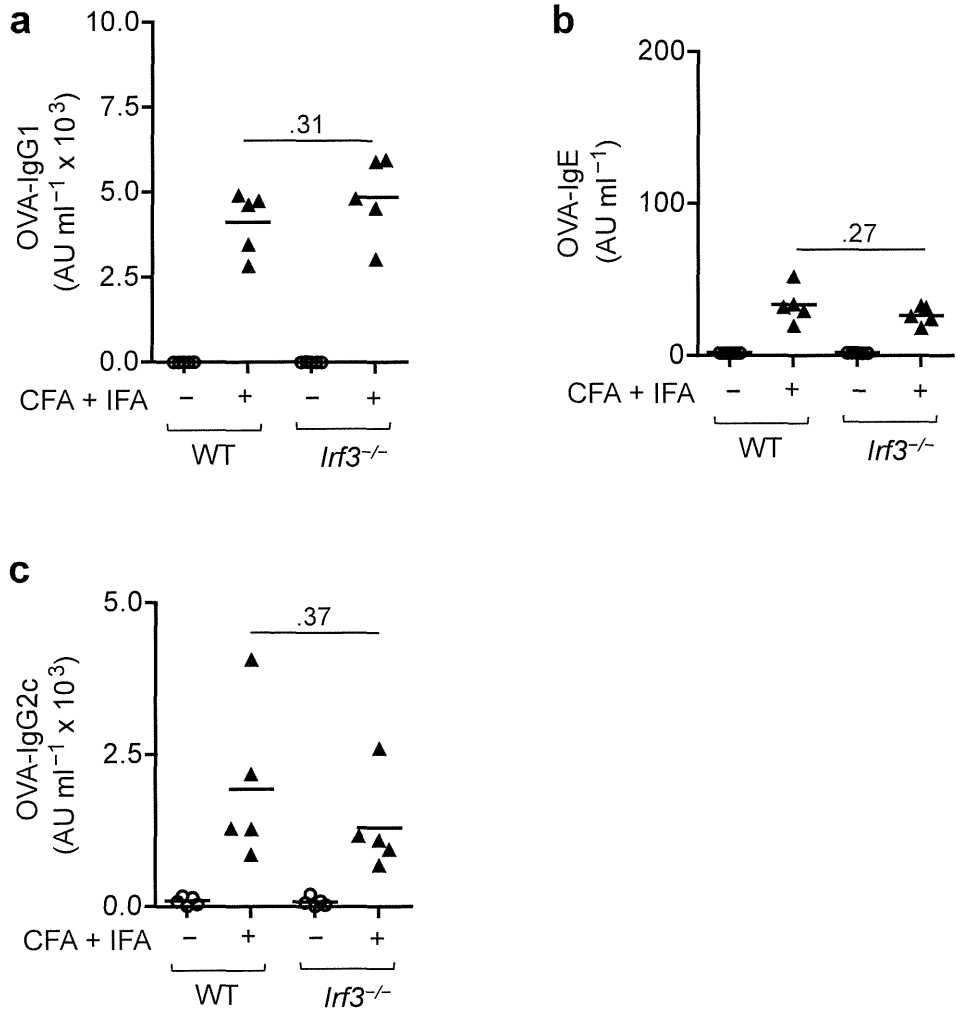

Supplementary Figure 11 *Irf3*$^{-/-}$ mice have normal immunization potential in response to Irf3-independent adjuvants. Serum OVA-specific IgG1 (**a**), IgE (**b**), and IgG2c (**c**) antibody titers measured on day 28 in WT and *Irf3*$^{-/-}$ mice immunized s.c. with OVA and CFA on day 0 and OVA and IFA on day 14, and boosted with OVA i.p. on day 21. *n*=5. Data are representative of one of two independent experiments. (AU, arbitrary unit).

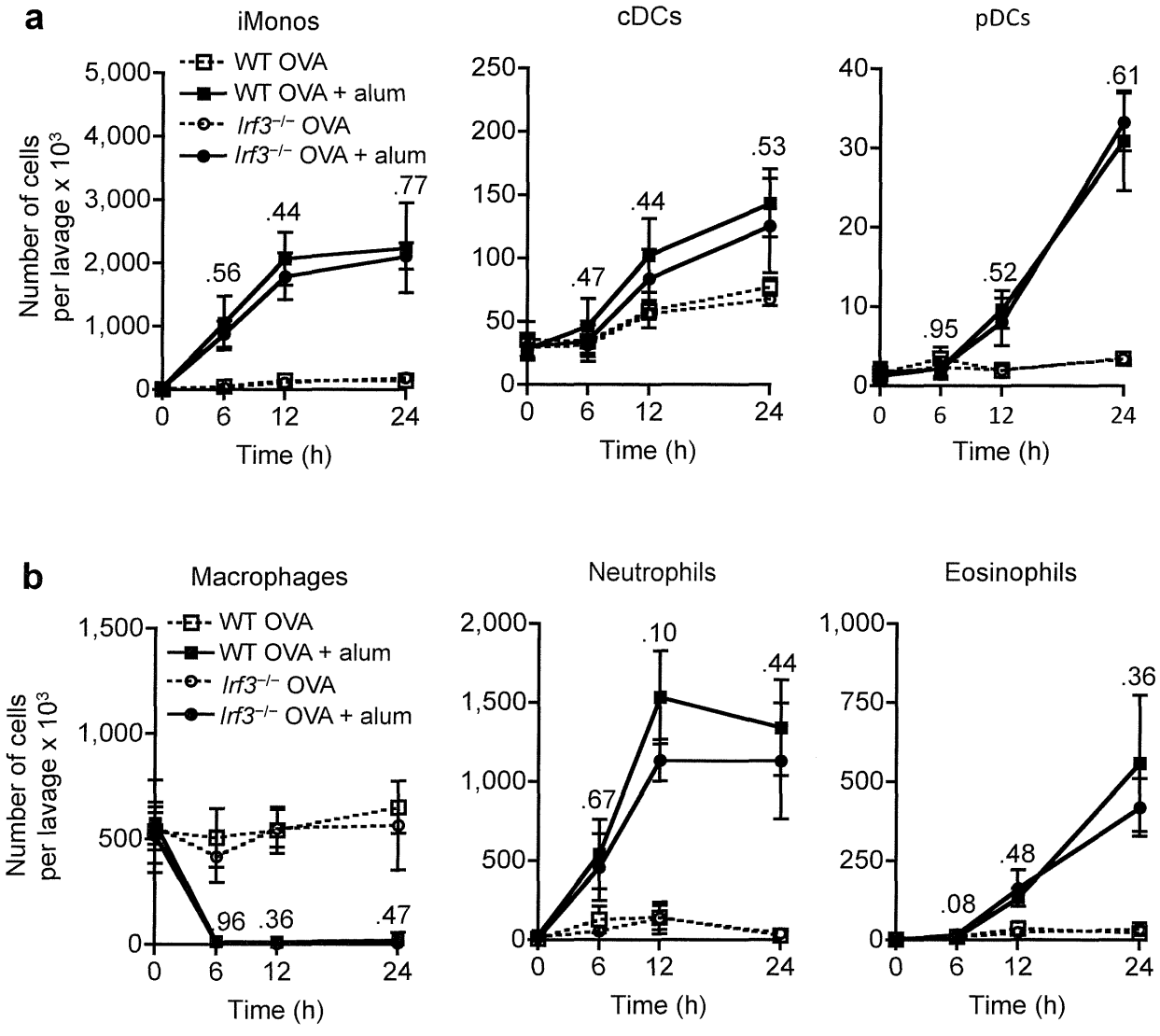

Supplementary Figure 12 Alum induces similar recruitment of innate immune cells in WT and *Irf3*$^{-/-}$ mice. Recruitment of innate immune cells through time in the peritoneal lavage fluid of WT and *Irf3*$^{-/-}$ mice treated i.p. with OVA or OVA and alum, assessed by flow cytometry. (**a**) We defined inflammatory monocytes (iMonos) as F4/80^{int} CD11b^{+} Ly6C^{+} Ly6G^{-} cells, conventional DCs (cDCs) as MHCII^{+} CD11c^{+} F4/80^{low} Ly6C^{-} cells, and plasmacytoid DCs (pDCs) as B220^{+} Ly6G^{+} CD11c^{int} F4/80^{low} cells. (**b**) We defined peritoneal macrophages as F4/80^{high} CD11b^{+} SSC^{high} cells, neutrophils as CD11b^{+} Ly6C^{+} Ly6G^{+} F4/80^{-} cells, and eosinophils as CD11b^{+} Ly6C^{int} Ly6G^{int} F4/80^{int} cells. *n*=5. Data are representative of one of four independent experiments.